SSRG International Journal of Mechanical Engineering
ISSN: 2348 – 8360 / https://doi.org/10.14445/23488360/IJME-V9I4P103

Volume 9 Issue 4, 18-29, April 2022

Original Article

Heat Transfer Enhancement through Perforated fin made by MMC by Reinforcing Aluminum with Graphite and Optimization of Design Parameters using Taguchi DOE Method

A. Kalyan Charan[1], R. Uday Kumar[2], B. Balunaik[3]

[1]*Department of Mechanical Engineering, Matrusri Engineering College, Hyderabad, India*
[2]*Department of Mechanical Engineering, Mahatma Gandhi Institute of Technology, Hyderabad, India*
[3]*Mechanical Engineering & Director of University Foreign Relations, JNTUH, Hyderabad, India.*

Received Date: 27 February 2022
Revised Date: 04 April 2022
Accepted Date: 16 April 2022

Abstract *- In comparison to other conventional fin materials, a stir casting process has been developed to produce aluminum–graphene (Al–Gr) metal matrix composites as a fin material. By Stir Casting, Fin Specimens were made with varied volume percentages of Graphite (5, 10, and 15%) in Al and Al as a base matrix. The rectangular fin's cross-sectional area was 40 mm x 3 mm, and its length was 100 mm. Experiments were conducted across a rectangular fin with lateral circular holes of varied porosities of 0.028, 0.038, 0.050, and 0.064, as well as variable flow rates from 4-7 m/s in 1 m/s increment. The design optimization parameters and associated levels were evaluated by using Taguchi L16 experimental design method. According to the findings, the heat transfer of the Al-Graphite nanocomposite was improved by increasing the volume percent of Gr particles. For porosity 0.064 friction factor and pressure drop, a combination of 85 percent Al-15 percent Gr produced a high heat transfer coefficient and enhanced heat transfer rate compared to standard aluminum. The optimal results were discovered for a fin composed of 85 percent Al - 15 percent Gr, which compares favorably to conventional fin materials while lighter and stronger than any of them. The fin's Porosity, velocity, and Composition yielded the best findings. According to research, the velocity, Porosity, and Composition have a greater influence on the heat transfer coefficient and Nusselt number.*

Keywords *- Heat transfer coefficient, Heat transfer, Nusselt number, Perforations, Taguchi.*

I. INTRODUCTION

Heat transfer [1] is increasing today due to advancements in many applications such as communications, mechatronics, and various electrical gadgets. Changes in the shape, size, quantity, and orientation of the holes [2] were also implemented to improve the thermal performance. The effects of the number and shape of the hollow fin on heat transmission via rectangular fins attached to a microchannel heat sink were studied using circular, rectangle, and trapezoidal cross-sectional areas of the perforation [3]. The number of depressions has a significant effect on the improvement, while the shape of the depressions has a little impact. Perforated fins appear to have better performance. Additionally, raising the porosity ratio results in greater efficacy. For a rectangular fin with lateral holes[19], the Reynolds number and perforation size have a greater influence on the Nusselt number [4] (square and circular).

Miniaturized segments and sub-devices, thermoelectric materials, and superior mechanical systems are only a few of the rapidly growing practical applications that can only be commercialized with the aid of MMCs [22]. Because of their superior mechanical and thermal characteristics, metal matrix composites (MMCs) [5] have many technical applications. These metal matrix composites require careful observation and tweaking of various crucial parameters [24] to give certain desired outputs. Such as weight %, volume fraction, size, form, and orientation are all factors that might affect the final composite sample's nature.

Aluminum matrix composites (AMCs) have lately attracted a lot of attention in commercial applications such as aerospace [20], automobiles, electronic/electrical equipment [6], and a variety of construction materials. aluminum has the

largest abundancy (among all metals) in the earth's crust, which gives it an edge over other significant metals like nickel, iron, magnesium, and chromium. Aside from that, aluminum has other distinguishing characteristics, including low density (which makes it exceptionally lightweight), resistance to corrosion, high thermal conductivity [21], malleability & ductility. Various reinforcing techniques have been investigated, including mixing the aluminum bulk with trace quantities of Al2O3, SiC [26], BN, TiB2, B4C, and other materials to generate AMCs with better mechanical, thermal characteristics [25]. Graphene and carbon nanotubes (CNTs) have recently been good AMC reinforcing materials [7] with improved electrical, thermal, lubricating, and tensile qualities. The Taguchi technique was used to achieve the goal of optimum values of design parameters in a heat exchanger.

We used aluminum as the metal matrix [23] and graphene as the reinforcement in this study. The stir Casting Process is a cost-effective method for producing Al-Graphite [12] composite. Rectangular fin with lateral circular perforations ranging in size from 12-18 mm in 2 mm increments (porosity are 0.028, 0.038, 0.050, and 0.064). The rectangular fin's cross-sectional area was 40 mm x 3 mm, its length was 100 mm, and the flow rate was 4 - 7 m/s in 1m/s increments. The design optimization characteristics and levels were examined using the Taguchi L16 experimental design method. It is vital to establish the economic benefits of heat transfer improvement in many practical applications. As a result, this research aims to reduce the number of experimental trials by utilizing Taguchi's experimental design to establish the heat transfer rate of perforated fins [13] and to find new design parameters and levels.

II. EXPERIMENTAL TEST SET UP AND DESIGN

A. Experimental Test SetUp

a) Stir Casting Apparatus Setup

The major components of the Stir casting equipment [8] are shown in Fig.1. Motor, Stirrer, Crucible, Melt Base Metal (Al), Reinforcement (Gr), Furnace, and Stirrer Blade.

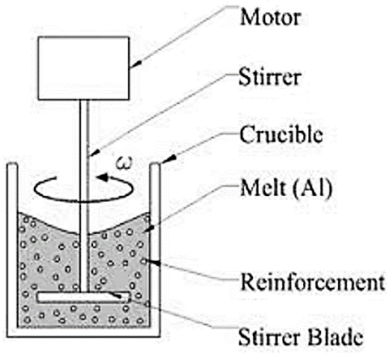

Fig. 1 Stir Casting Apparatus

Stirring duration and pace are critical; otherwise, reinforcement would settle to the bottom or on one side. The reinforcing material is injected into the matrix to enhance or degrade its characteristics [9]. This research is focused on composites of various compositions. Figure 2 depicts a stir casting furnace (b). For improved reinforcement bonding with the matrix, the stirrer depicted in Fig.(h) is used to reinforce the reinforcement in the matrix.

Fig. 2 Stir casting procedure (a) Aluminum (b) Furnace (c) Cast Al Plates (d) Weight Machine (e) Graphite Powder (f) Measured Graphite Powder (g) Stirrer (h)Stirrer with the furnace (i) Al-Gr MMC Plates

The process described above is employed to make components in the aluminum matrix [10] with varied Gr reinforcement proportions of 5 percent, 10 percent, and 15 percent in 95 percent Al, 90 percent Al, and 85 percent Al. Table 1. lists the compositions that were created

Table 1. The Compositions

S.No	Composition (%)
1	AL
2	95%AL+5% Gr
3	90%AL+10% Gr
4	85%AL+15% Gr

b) Pin Fin Apparatus Setup

Fig.3 depicts the experimental setup. The Duct, Heater, Data Unit, and Plate Fin are all essential components of the arrangement.

Fig. 3 Pin fin Apparatus

In the rectangular duct of the pin fin apparatus illustrated in Fig.3. a fin with a rectangular cross-section of length=100mm, width=40mm, and thickness t=3mm is fitted. The base of the fin is attached to a heater, which is used to heat the fin. Temperature sensors are installed on the fin's surface to measure the temperature. A draught fan is installed in the duct to regulate airflow with the aid of a regulator. An anemometer has been provided to determine the air velocity via the duct. A digital wattmeter has been given to know the heater's input power.

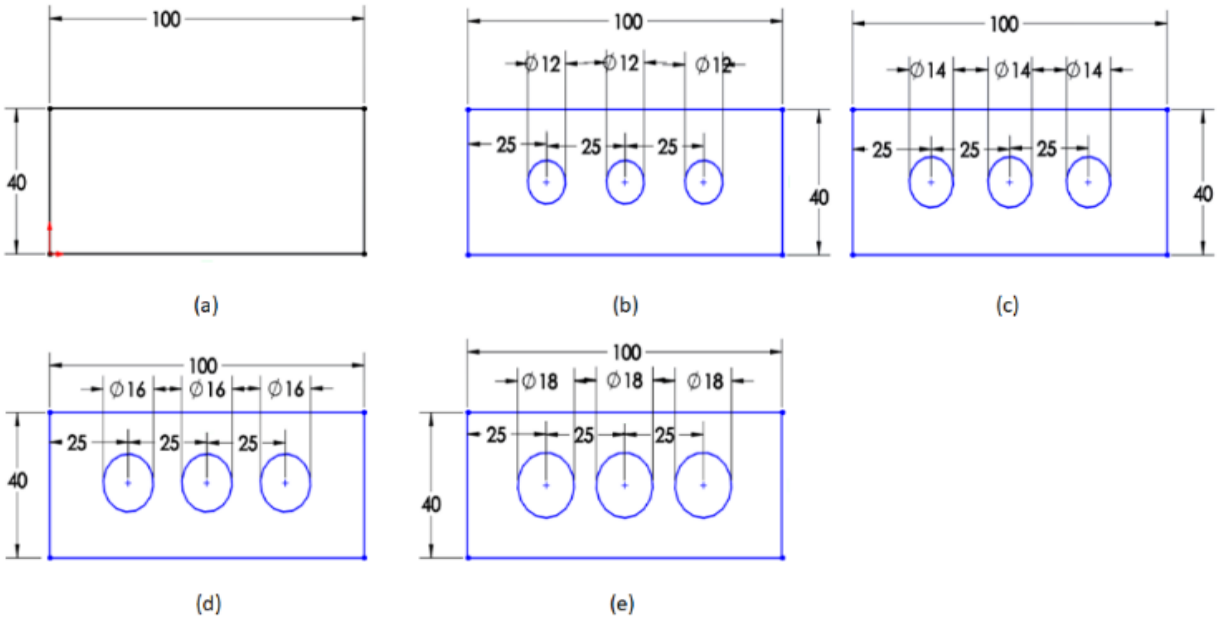

Fig. 4 (A) Types of fins (a) Plane fin, Perforated fins (3 perforations) (b) porosity =0.028 (c) porosity =0.038 (d) porosity =0.050 and (e) porosity =0.064

Fig. 4 (B) Types of fins (a) Perforated 85%Al-15%Gr fins (b) Perforated 90%Al-10%Gr fins (c) Perforated 95%Al-5%Gr fins. In the above three cases, perforations vary from 12mm – 18mm in diameter

Fig. 4(A) & 4(B) depicts the many types of fins, such as plane and perforated fins [18]. Perforations of various porosities and compositions are

- No. of perforations: 3
- Type of fin: Without perforation & With perforation
- Composition: Al, 95%Al+5% Gr, 90%Al+10% Gr & 85%Al+15% Gr
- Size of perforation: 12, 14, 16 & 18
- Porosity: 0.028, 0.038, 0.05 & 0.064

B. Experimental Design

Taguchi Technique: Because of its wide variety of applications, the Taguchi approach is commonly used in industrial and engineering disciplines. The Taguchi technique is the most widely used method for enhancing design parameters [11]. The approach was initially offered to improve product quality by combining statistical and technical considerations. This method is founded on two key concepts: The first is that quality losses must be identified as deviations from the aims, not arbitrary specifications, and the second is that achieving high system quality levels meticulously implies quality to be built into the product. Taguchi advocates a three-stage procedure to achieve required product quality via design: system design, parameter design, and tolerance design [15].

The use of Signal-to-Noise (S/N) ratios for the same phases of the analysis is strongly recommended by Taguchi. The S/N ratio is a loss function-connected concurrent quality measurement method. The loss associated with the procedure can be avoided by optimizing the S/N ratio. From the diversity in the findings, the S/N ratio identifies the most resilient set of operational circumstances. It is handled as an experiment response parameter. The experimental data is converted to a signal-to-noise ratio (S/N). Depending on the sort of features, several S/N ratios are available. Eqs classify the S/N ratio features into three categories.

Smaller is the better characteristic: $\frac{S}{N} = -10log\left(\frac{1}{n}\sum_{i=1}^{n} Y^2\right)$

Nominal the better characteristic: $\frac{S}{N} = -10log\left(\frac{1}{n}\sum_{i=1}^{n} \frac{\bar{Y}}{S_{yi}^2}\right)$

Larger the better characteristic $\frac{S}{N} = -10log\left(\frac{1}{n}\sum_{i=1}^{n} \frac{1}{Y_i^2}\right)$

$\bar{Y}$ is the average of the observed data. S_{yi}^2 represents Y variation, The number of observations is denoted by the letter n., and Y represents the observed data. As indicated in Table 2. the number of holes on the lateral surface of the fins (Porosity), velocity, and fin thickness were chosen as control factors with their values.

Table 2. Control Parameters and their Levels

Control Parameter	Level I	Level II	Level III	Level IV
Velocity	4	5	6	7
Porosity	0.028	0.038	0.050	0.064
Composition	Al	95%Al+ 5% Gr	90%Al+ 10% Gr	85%Al+ 15% Gr

Table 3. Orthogonal array L_{16}

Expt. Trials	Velocity(V)	Porosity (∅)	Composition (%)
1	4	0.028	Al
2	4	0.038	95%Al+5% Gr
3	4	0.050	90%Al+10% Gr
4	4	0.064	85%Al+15% Gr
5	5	0.028	95%Al+5% Gr
6	5	0.038	Al
7	5	0.050	85%Al+15% Gr

8	5	0.064	90%Al+10% Gr
9	6	0.028	90%Al+10% Gr
10	6	0.038	85%Al+15% Gr
11	6	0.050	Al
12	6	0.064	95%Al+5% Gr
13	7	0.028	85%Al+15% Gr
14	7	0.038	90%Al+10% Gr
15	7	0.050	95%Al+5% Gr
16	7	0.064	Al

Table 3. shows the Taguchi experimental design strategy that was chosen. This strategy is the most appropriate for the optimal working circumstances under investigation. ACCORDING TO THE TAGUCHI TECHNIQUE, an L_{16} orthogonal array can deliver good experimental performance with a minimum number of experimental trials. For each combination of control parameters, the Nusselt number was computed using the experimental method, and the S/N ratio was determined.

C. Data Processing

The heat delivered to the flow by forced convection in steady-state circumstances is the net heat transfer rate Q. Eq. may be used to compute the convective heat transfer between the fin with perforations [16] and fin without perforations arrays. $Q = h\ A_T\left[T_s - \left(\frac{T_{Out}+T_{in}}{2}\right)\right]$

The area A_T in Eq. is the entire surface area of heat transfer that comes into touch with the fluid moving through the duct.

$A_T = N_f\left[2HL + Lt - \left(\frac{\pi}{2}d^2\right)N_p + \pi dtN_p\right]$ Perforated fin

$A_T = N_f[2Ht + 2HL + Lt]$ Solid fin

L and H are the fin's length and height, respectively, while t is its thickness and N_f is the number of fins.

The dimensionless groups are determined in the following manner.: $Nu = \frac{h\ L_c}{K_a}$

The Nusselt Number value (Nu) is based on the overall heat transfer area. It simulates the influence of surface area differences and flow disorder caused by the fin shape on heat transfer. The Reynolds number (Re) is calculated using the duct's hydraulic diameter and averaged flow entrance velocity. $Re = \frac{\rho_a V D_h}{\mu}$

The volume of perforations [17] divided by the volume of solid fins is known as Porosity. Porosity $\emptyset = \frac{Volume_{Void}}{Volume_{Solid}}$

The mean temperature is used in all computations to derive the values of thermophysical characteristics of air. $T_{Mean} = \frac{T_{Out}+T_{In}}{2}$

III. RESULT AND DISCUSSION

Table 4. shows the computed experimental values for the fin with and without perforation, as well as the outcomes.

Table 4. Experimental values for the fin with and without perforation

Type of fin	Velocity (V)	Porosity (∅)	Composition (%)	Average Nusselt number (Nu)	Average heat transfer coefficient (h)	Heat transfer (Q)	Friction Factor	Pressure Drop
Without perforation	4	-	Al	64.7	14.97	10.40	0.0089	0.0355
With perforation	4	0.028	Al	62.1	15.70	11.18	0.0093	0.0371
With perforation	4	0.038	95%Al+5%Gr	61.1	15.99	11.26	0.0094	0.0377
With perforation	4	0.050	90%Al+10%Gr	59.9	16.34	11.44	0.0096	0.0385
With perforation	4	0.064	85%Al+15%Gr	58.6	16.76	11.69	0.0099	0.0394
With perforation	5	0.028	95%Al+5%Gr	68.9	17.42	12.25	0.0083	0.0332
With perforation	5	0.038	Al	67.8	17.74	12.74	0.0084	0.0337
With perforation	5	0.050	85%Al+15%Gr	66.5	18.13	12.63	0.0086	0.0344
With perforation	5	0.064	90%Al+10%Gr	65.0	18.60	13.19	0.0088	0.0353
With perforation	6	0.028	90%Al+10%Gr	75.0	18.96	13.24	0.0076	0.0303
With perforation	6	0.038	85%Al+15%Gr	73.8	19.31	13.43	0.0077	0.0308
With perforation	6	0.050	Al	72.4	19.73	14.33	0.0079	0.0314
With perforation	6	0.064	95%Al+5%Gr	70.8	20.25	14.61	0.0081	0.0322
With perforation	7	0.028	85%Al+15%Gr	80.6	20.37	16.85	0.0070	0.0280
With perforation	7	0.038	90%Al+10%Gr	79.3	20.75	14.63	0.0071	0.0285
With perforation	7	0.050	95%Al+5%Gr	77.8	21.20	15.23	0.0073	0.0291
With perforation	7	0.064	Al	76.1	21.76	15.96	0.0075	0.0298

Table 5. illustrates the percentage increase in heat transfer coefficient h and heat transfer rate of perforated fins over plane fins.

Table 5. Percentage increase in heat transfer coefficient and heat transfer rate of perforated fin over the plane fin

Type of fin	Velocity (V)	Porosity (∅)	Composition (%)	Percentage increase 'h' over plan fin	Percentage increase 'Q' over plan fin
Without perforation	4	-	Al	-	-
With perforation	4	0.028	Al	4.84	7.44
With perforation	4	0.038	95%Al+5%Gr	6.77	8.22
With perforation	4	0.050	90%Al+10%Gr	9.12	9.94
With perforation	4	0.064	85%Al+15%Gr	11.97	12.36
With perforation	5	0.028	95%Al+5%Gr	16.33	17.79
With perforation	5	0.038	Al	18.47	22.44
With perforation	5	0.050	85%Al+15%Gr	21.07	21.39
With perforation	5	0.064	90%Al+10%Gr	24.24	26.75
With perforation	6	0.028	90%Al+10%Gr	26.65	27.28
With perforation	6	0.038	85%Al+15%Gr	28.97	29.09
With perforation	6	0.050	Al	31.81	37.70
With perforation	6	0.064	95%Al+5%Gr	35.25	40.46
With perforation	7	0.028	85%Al+15%Gr	36.08	61.98
With perforation	7	0.038	90%Al+10%Gr	38.58	40.57
With perforation	7	0.050	95%Al+5%Gr	41.63	46.41
With perforation	7	0.064	Al	45.33	53.44

We may deduce from Table 5. that perforating a plane fin while altering velocity, perforation size, and Composition enhances the percentage increase in convective heat transfer coefficient and heat transfer rate. We used the Taguchi technique to discover the best ideal design. The S/N ratio for the L_{16} orthogonal array is shown in Table 6. All of the experiential values in the Taguchi technique are derived with the assumption that the larger, the better.

A. Taguchi Analysis

Heat Transfer Coefficient h, Heat Transfer Rate vs. Velocity(V), Porosity (∅), and Material Composition as a percentage increase.

Table 6. S/N ratio for L16 orthogonal array (heat transfer coefficient h, heat transfer rate versus Velocity(V), Porosity (∅), Material composition)

Exp. Trials	Velocity (V)	Porosity (∅)	Composition (%)	Percentage increase over plan fin %h	SNRA1 for '%h'	Percentage increase over plan fin %Q	SNRA2 for '%Q'	SNRA3 for '%h & %Q'
1	4	0.028	Al	4.84	13.7049	7.44	17.4363	15.1816
2	4	0.038	95%Al+5%Gr	6.77	16.6075	8.22	18.2957	17.3701
3	4	0.050	90%Al+10%Gr	9.12	19.1957	9.94	19.9439	19.5537
4	4	0.064	85%Al+15%Gr	11.97	21.5588	12.36	21.8371	21.6957
5	5	0.028	95%Al+5%Gr	16.33	24.2617	17.79	25.0013	24.6158
6	5	0.038	Al	18.47	25.3277	22.44	27.0193	26.0917
7	5	0.050	85%Al+15%Gr	21.07	26.4745	21.39	26.6060	26.5397
8	5	0.064	90%Al+10%Gr	24.24	27.6890	26.75	28.5474	28.0970
9	6	0.028	90%Al+10%Gr	26.65	28.5138	27.28	28.7178	28.6146
10	6	0.038	85%Al+15%Gr	28.97	29.2395	29.09	29.2754	29.2574
11	6	0.050	Al	31.81	30.0510	37.70	31.5271	30.7266
12	6	0.064	95%Al+5%Gr	35.25	30.9437	40.46	32.1413	31.5013
13	7	0.028	85%Al+15%Gr	36.08	31.1458	61.98	35.8450	32.8886
14	7	0.038	90%Al+10%Gr	38.58	31.7266	40.57	32.1639	31.9397
15	7	0.050	95%Al+5%Gr	41.63	32.3873	46.41	33.3323	32.8341
16	7	0.064	Al	45.33	33.1268	53.44	34.5576	33.7835

S/N Response Table 7: Percentage increase in convective heat transfer coefficient over plan fin vs. velocity (v), Porosity (∅), and Composition (%)

Taguchi Analysis: Percentage increase over plan fin h versus velocity (v), Porosity (∅), Composition (%)

Table 7. Response Table for Signal to Noise Ratios: Larger is better

Level	Velocity(v)	Porosity (Ø)	Composition (%)
1	17.77	24.41	27.10
2	25.94	25.73	26.78
3	29.69	27.03	26.05
4	32.10	28.33	25.55
Delta	14.33	3.92	1.55
Rank	1	2	3

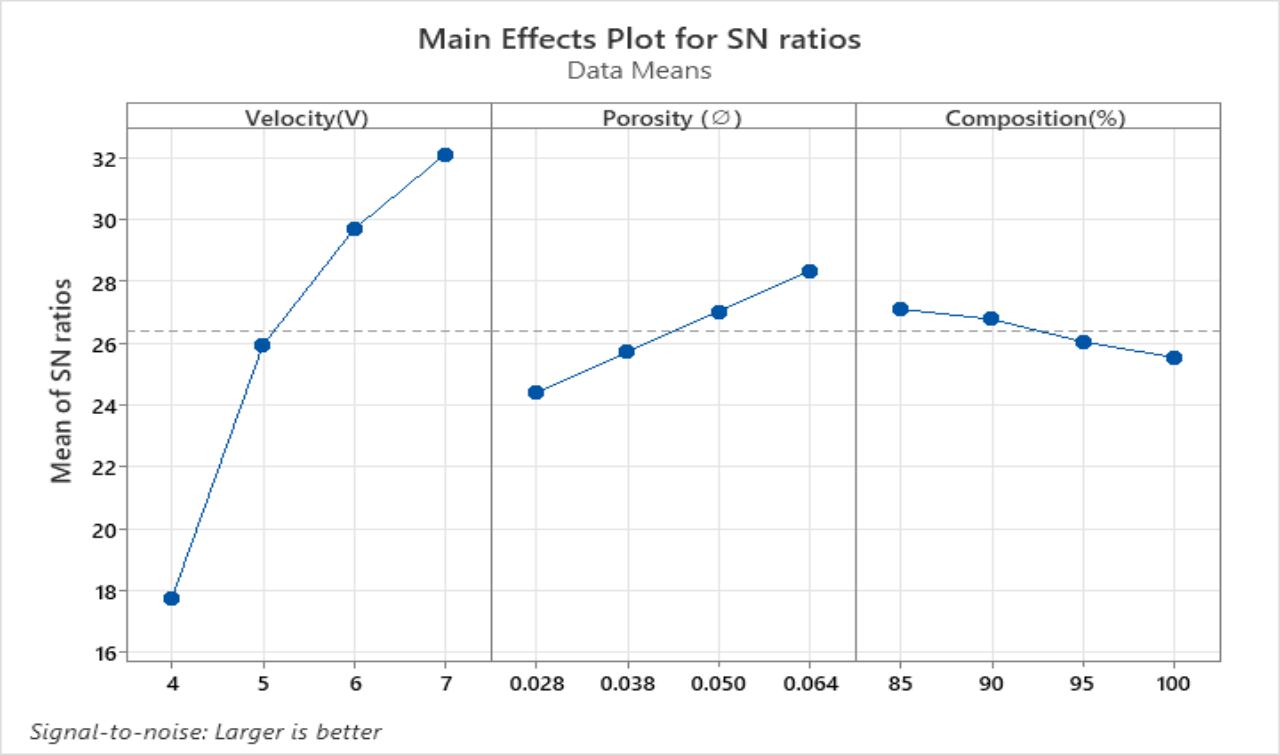

Fig. 5 Signal to Noise Ratios (% increase over plan fin h versus velocity (v), Porosity (Ø), Composition (%))

According to Fig. 5, the optimum level design made this possible for a percentage increase in convective heat transfer coefficient over plan fin is V4, Ø4 & for Composition4, with the values of each parameter being V4, i.e., Velocity diameter is 7 m/s, Ø4, i.e., Porosity of fin is 0.064mm, i.e., 18mm perforation diameter, and Composition4, i.e., Composition of the fin is 85%Al+15%Gr.

S/N Response Table 8: percentage increase of heat transfer Q over plan fin vs. velocity (v), Porosity (Ø), and Composition (%)

Taguchi Analysis: percentage increase heat transfer Q over plan fin versus velocity (v), Porosity (Ø), Composition (%).

Table 8. Response Table for Signal to Noise Ratios: Larger is better

Level	Velocity(v)	Porosity (Ø)	Composition (%)
1	19.38	26.75	28.39
2	26.79	26.69	27.34
3	30.42	27.85	27.19
4	33.97	29.27	27.64
Delta	14.60	2.58	1.20
Rank	1	2	3

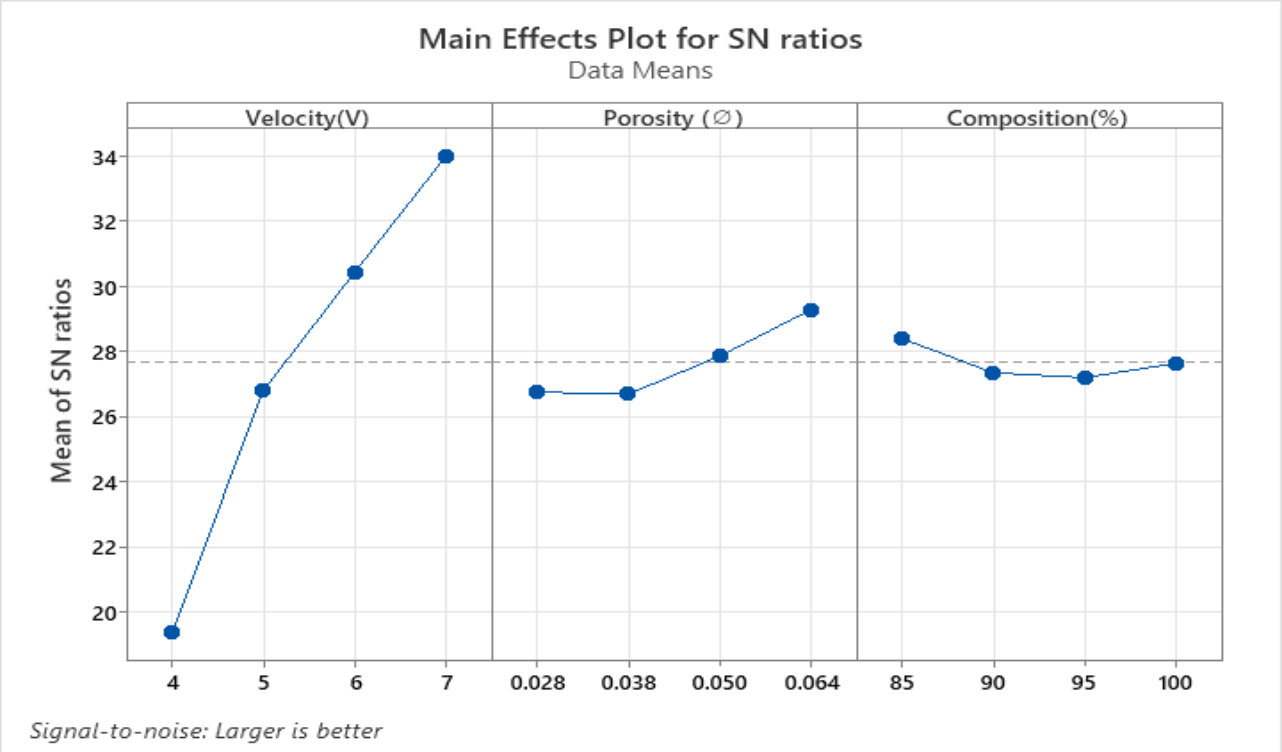

Fig. 6. Signal to Noise Ratios (% increase of heat transfer Q over plan fin versus velocity (v), Porosity (Ø) & Composition (%))

According to Fig. 6, the optimum level design made this possible for a percentage increase in heat transfer Q over plan fin is V4, Ø4 & for Composition4, with the values of each parameter being V4, i.e., Velocity diameter is 7 m/s, Ø4, i.e., Porosity of fin is 0.064mm, i.e., 18mm perforation diameter, and Composition4, i.e., Composition of the fin is 85%Al+15%Gr.

S/N Response Table 9: Percentage increase over plan fin h, % increase over plan fin Q vs. Velocity(v), Porosity (Ø), and Composition (%)

Taguchi Analysis: Percentage increase over plan fin h, % increase over plan fin Q versus Velocity(v), Porosity (Ø), Composition (%).

Table 9. Response Table for Signal to Noise Ratios: Larger is better

Level	Velocity(v)	Porosity (Ø)	Composition (%)
1	18.45	25.33	27.60
2	26.34	26.16	27.05
3	30.03	27.41	26.58
4	32.86	28.77	26.45
Delta	14.41	3.44	1.15
Rank	1	2	3

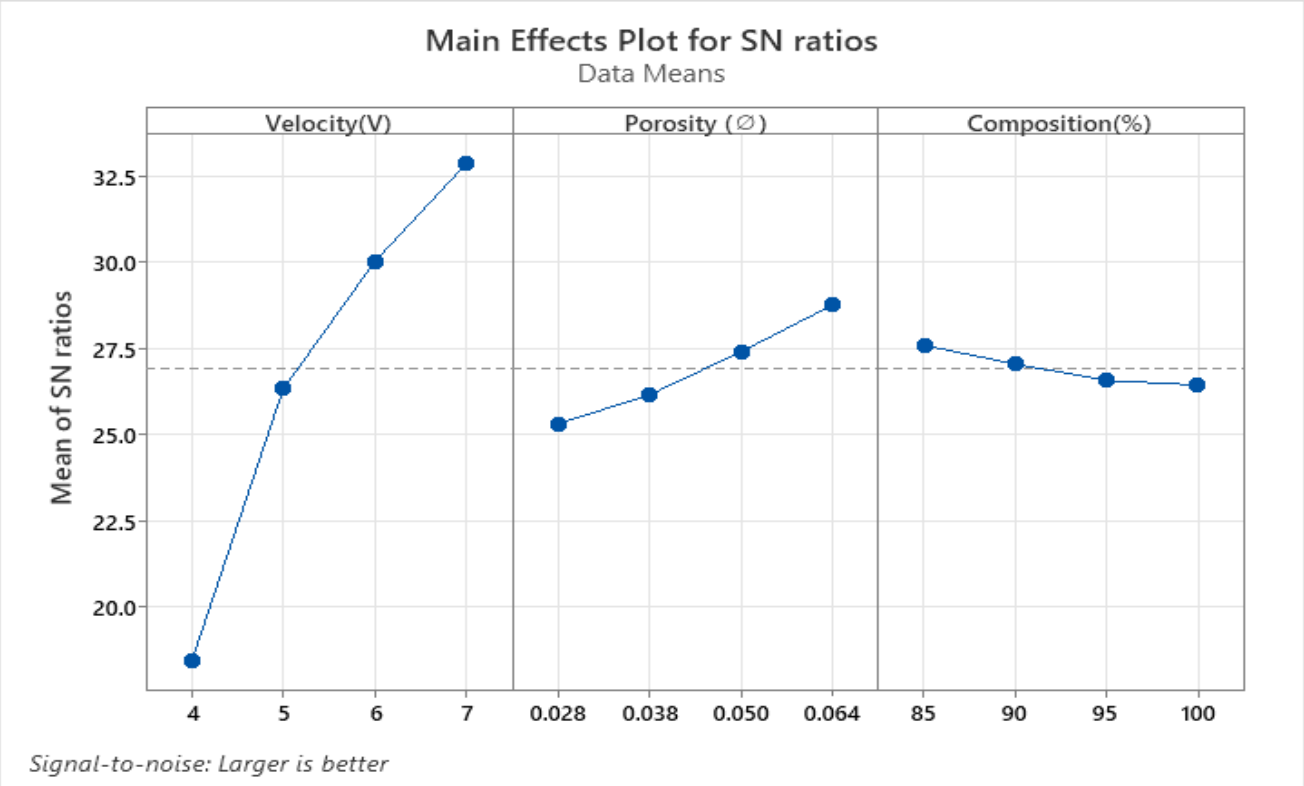

Fig. 7 Signal to Noise Ratios (% increase over plan fin h, % increase over plan fin Q versus Velocity(v), Porosity (Ø), Composition (%))

According to Fig. 7, the optimum level design made this possible for a percentage increase in heat transfer coefficient h, heat transfer rate Q over plan fin is V4, Ø4 & for Composition4, with the values of each parameter being V4, i.e., Velocity diameter is 7 m/s, Ø4, i.e., Porosity of fin is 0.064mm, i.e., 18mm perforation diameter, and Composition4, i.e., Composition of the fin is 85%Al+15%Gr

The S/N ratio for the L16 orthogonal array is shown in Table 10. All of the experiential values in the Taguchi approach are computed with the assumption that the larger, the better. The friction factor [14] and pressure drop experienced values will be set to the maximum in this study.

Table 10. S/N ratio for L16 orthogonal array for friction factor and pressure drop

Type of fin	Velocity (V)	Porosity (Ø)	Composition (%)	Friction Factor	SNRA4 for Friction Factor	Pressure Drop	SNRA5 for Pressure Drop
With perforation	4	0.028	Al	0.0093	-40.6303	0.0371	-28.6125
With perforation	4	0.038	95%Al+5%Gr	0.0094	-40.5374	0.0377	-28.4732
With perforation	4	0.050	90%Al+10%Gr	0.0096	-40.3546	0.0385	-28.2908
With perforation	4	0.064	85%Al+15%Gr	0.0099	-40.0873	0.0394	-28.0901
With perforation	5	0.028	95%Al+5%Gr	0.0083	-41.6184	0.0332	-29.5772
With perforation	5	0.038	Al	0.0084	-41.5144	0.0337	-29.4474
With perforation	5	0.050	85%Al+15%Gr	0.0086	-41.3100	0.0344	-29.2688
With perforation	5	0.064	90%Al+10%Gr	0.0088	-41.1103	0.0353	-29.0445
With perforation	6	0.028	90%Al+10%Gr	0.0076	-42.3837	0.0303	-30.3711
With perforation	6	0.038	85%Al+15%Gr	0.0077	-42.2702	0.0308	-30.2290
With perforation	6	0.050	Al	0.0079	-42.0475	0.0314	-30.0614
With perforation	6	0.064	95%Al+5%Gr	0.0081	-41.8303	0.0322	-29.8429
With perforation	7	0.028	85%Al+15%Gr	0.0070	-43.0980	0.0280	-31.0568
With perforation	7	0.038	90%Al+10%Gr	0.0071	-42.9748	0.0285	-30.9031
With perforation	7	0.050	95%Al+5%Gr	0.0073	-42.7335	0.0291	-30.7221
With perforation	7	0.064	Al	0.0075	-42.4988	0.0298	-30.5157

S/N Response Table 11: Friction Factor vs. Velocity(v), Porosity (Ø), and Composition (%)

Taguchi Analysis: Friction Factor versus Velocity(v), Porosity (Ø), Composition (%)

Table 11. Response Table for Signal to Noise Ratios: Larger is better

Level	Velocity(v)	Porosity (Ø)	Composition (%)
1	-40.40	-41.93	-41.69
2	-41.39	-41.82	-41.71
3	-42.13	-41.61	-41.68
4	-42.83	-41.38	-41.67
Delta	2.42	0.55	0.03
Rank	1	2	3

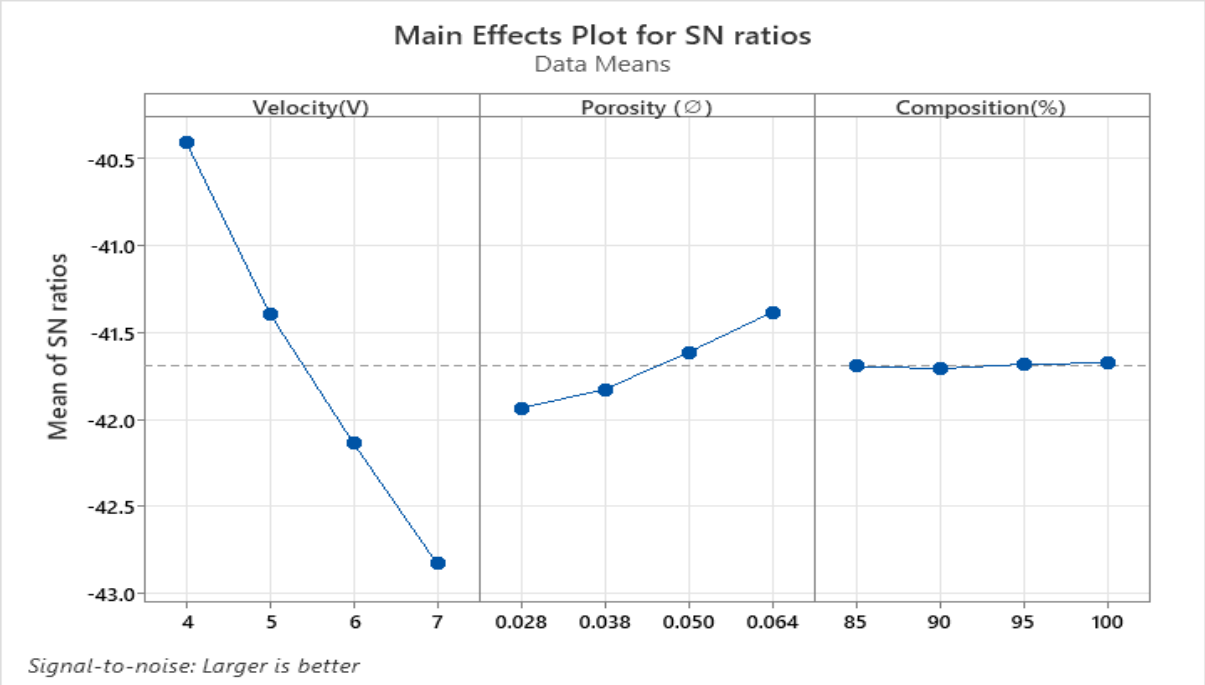

Fig. 8 Signal to Noise Ratios (Friction Factor versus Velocity(v), Porosity (Ø), Composition (%))

Fig 8 is an excellent demonstration that the friction factor decreases when velocity rises. At low speeds, the friction factor is significant, while at high speeds, it is low. The friction factor increases as the porosity increases, reaching a maximum at 0.064 and a minimum at 0.028, while the composition proportion does not affect the friction factor.

S/N Response Table 12: Pressure drop vs. Velocity(v), Porosity (Ø), and Composition (%)

Taguchi Analysis: Pressure drop versus velocity (v), Porosity (Ø), Composition (%)

Table 12. Response Table for Signal to Noise Ratios: Larger is better

Level	Velocity(v)	Porosity (Ø)	Composition (%)
1	-28.37	-29.90	-29.66
2	-29.33	-29.76	-29.65
3	-30.13	-29.59	-29.65
4	-30.80	-29.37	-29.66
Delta	2.43	0.53	0.01
Rank	1	2	3

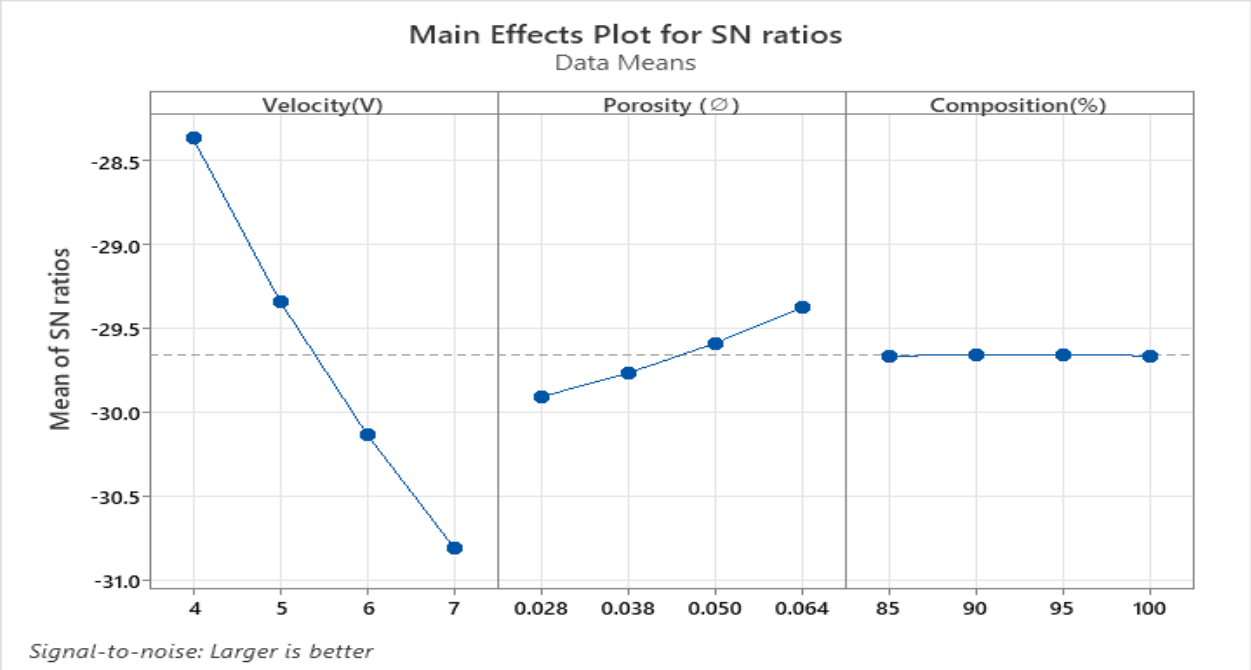

Fig. 9 Signal to Noise Ratios (Pressure drop versus velocity (v), Porosity (Ø), Composition (%))

Fig 9. illustrates when velocity rises, the pressure drop reduces. The pressure drop is high at low speeds and minimal at high speeds. The pressure drop increases as the porosity increases, reaching a maximum at 0.064 and a minimum at 0.028, while the composition proportion does not affect the pressure drop.

IV. CONCLUSION

According to the findings, perforating a plane fin and altering velocity, Porosity, and Composition enhances the heat transfer coefficient, heat transfer rate, friction factor, and pressure drop. With the Taguchi Method, we can achieve the optimal answer with fewer trials. According to the research done on Taguchi L16 orthogonal arrays, the velocity of the fin is the most important factor determining the heat transfer coefficient, followed by Porosity and then the Composition of fins. The highest heat transfer rate limit is practicable for 3 mm fin thickness and 7 m/s airflow velocities, 0.064 porosity in fin, and the Composition 85%Al+15%Gr. As a result, it's reasonable to conclude that heat transfer can be efficiently increased by enhancing these parameters. The pressure drop diminishes as the velocity increases, and the friction factor lowers. Because of the friction factor, the pressure loss is considerable at low speeds and low at high speeds. The friction factor, pressure drop, increases as the porosity increases, with a maximum at 0.064 and a minimum at 0.028. At the same time, the proportion of Composition does not affect the friction factor or pressure drop. Consequently, we believe that using the L_{16} Orthogonal Array Method will yield an incomparable result with fewer trials and is also cost-effective.

ACKNOWLEDGMENT

The author (Mr.A.Kalyan Charan, Assistant Professor, Dept. of Mechanical Engineering, and MECS) wishes to express his gratitude to the management and principal of Matrusri Engineering College (MECS) for their encouragement and permission to conduct this research.

REFERENCES

[1] S.Pradeep Narayanan, G. Venkatarathnam, Analysis of the Performance of Heat Exchangers Used in Practical Micro Miniature Refrigerators, Cryogenics. 39(6) (1999) 517-527.

[2] Banerjee R, Karve M, Evaluation of Enhanced Heat Transfer within a Four-Row Finned Tube Array of an Air-Cooled Steam Condenser, Numer Heat Tr A-Appl. 61 (2012) 735–753

[3] Maha A. Hussein, Vinous M. Hameed, Hussein T. Dhaiban, An Implementation Study on a Heat Sink with Different Fin Configurations Under Natural Convective Conditions, Case Studies in Thermal Engineering. 30 (2022) 101774.

[4] Yakar, Gülay & Karabacak, Rasim, Effects of Different Fin Spacings on the Nusselt Number and Reynolds Number in Perforated Finned Heat Exchangers, Heat Transfer Engineering. 32 (2011) 399-407.

[5] M. Penchal Reddy, Vyasaraj Manakari, Gururaj Parande, R.A. Shakoor, A.M.A. Mohamed, M. Gupta, Structural, Mechanical and Thermal Characteristics of Al-Cu-Li Particle Reinforced Al-Matrix Composites Synthesized by Microwave Sintering and Hot Extrusion, Composites Part B: Engineering. 164 (2019) 485-492.

[6] Surappa, Mirle, Aluminium Matrix Composites: Challenges and Opportunities, Sadhana. 28 (2003) 319-334.

[7] Kwon, Hansang & Park, Dae & Silvain, J.-F & Kawasaki, Akira, Investigation of Carbon Nanotube Reinforced Aluminum Matrix Composite Materials, Composites Science and Technology. 70 (2010) 546-550.

[8] V. Mohanavel, K. Rajan, P.V. Senthil, S. Arul, Mechanical Behavior of Hybrid Composite (AA6351+Al2O3+Gr) Fabricated by Stir Casting Method, Materials Today: Proceedings. 4(2) (2017) 3093-3101.

[9] Dipen Kumar Rajak, Durgesh D. Pagar, Ravinder Kumar, Catalin I. Pruncu, Recent Progress of Reinforcement Materials: A Comprehensive Overview of Composite Materials, Journal of Materials Research and Technology. 8(6) (2019) 6354-6374.

[10] Arunkumar K N, Dr. G B Krishnappa, Mechanical Properties of Aluminum Metal Matrix Composites – A Review, International Journal of Engineering Research & Technology (IJERT). 11(03) (2022).

[11] Patyal VS, Modgil S, Maddulety K, Application of Taguchi Method of Experimental Design for Chemical Process Optimisation: A Case Study, Asia-Pacific Journal of Management Research and Innovation. 9(3) (2013) 231-238.

[12] B.K.Prasad, The Significance of the Matrix Microstructure on the Solid Lubrication Characteristics of Graphite in Aluminum Alloys, Materials Science and Engineering. 144(12) (1991).

[13] Kiwan S, Al-Nimr M. A, Using Porous Fins for Heat Transfer Enhancement, Journal of Heat Transfer. 5 (2001) 123-790

[14] J. Yun and K. Lee, Influence of Design Parameters on the Heat Transfer and Flow Friction Characteristics of the Heat Exchanger with Slit Fins, International Journal of Heat and Mass Transfer. 43 (2000) 2529-2539.

[15] Nevin Celik, Gongur Pusat, Emre Turgut, Application of Taguchi Method and Grey Relational Analysis on a Tubulated Heat Exchanger, International Journal of Thermal Sciences. 124 (2018) 85-97.

[16] Karima Boukhadiaa, Houari Ameura, Djamel Sahelc, Mohamed Bozitb, Effect of the Perforation Design on the Fluid Flow and Heat Transfer Characteristics of a Plate Fin Heat Exchanger, International Journal of Thermal Sciences. 126 (2018) 172–180.

[17] Thamir K. Ibrahim, Marwah N. Mohammed, Mohammed Kamil Mohammed, G. Najafi, Nor Azwadi Che Sidik, Firdaus Basrawi, Ahmed N Abdalla, S.S. Hoseini, Experimental Study on the Effect of Perforations Shapes on Vertical Heated Fins Performance Under Forced Convection Heat Transfer, International Journal of Heat and Mass Transfer. 118 (2018) 832–846.

[18] Waleed Al-Salami, Amer Al-Damook, H.M. Thompson, A Numerical Investigation of the Thermal-Hydraulic Characteristics of Perforated Plate-Fin Heat Sinks, International Journal of Thermal Sciences. 121 (2017) 266-277.

[19] Akhilesh Kumar Singh, Rajiv Varshney, Experimental Investigation on Rectangular Fins with Holes in Natural Convection, International Journal of Engineering Development and Research. 5(4) (2017) 157-166.

[20] Assel Sakanova, Heat Transfer Enhancement of Perforated Pin Heat Sink in Future Aircraft Applications, Applied Thermal Engineering. 124 (2017) 315–326.

[21] R. Suresh, C. Srinivas, Sneha. H. Doria, Experimental Investigation of Thermal Conductivity of Aluminium Metal Matrix Composites, International Journal of Engineering Development and Research. 7(3) (2019).

[22] Akhil R, A Study on Recent Trends in the Applications of Metal Matrix Composites, International Journal for Research in Applied Science & Engineering Technology. 6(5) (2018) 172-180.

[23] Siddharth Swarnkar, Ashish Kumar Upadhyay, Comparison of Heat Transferring Fins of Conventional Aluminum and Metal Matrix Composites, J. Technological Advances and Scientific Res, 2(2) (2016) 131-134.

[24] Lalit M Manocha, High Performance Carbon–Carbon Composites, Materials Science. 28 (1&2) (2003) 349–358.

[25] Preetkanwal Singh Bains, Sarabjeet Singh Sidhu & H. S. Payal, Fabrication and Machining of Metal Matrix Composites A Review, Materials and Manufacturing Processes. (2015) 1–21.

[26] Y. Pratapa Reddy, B. Jithendra Kumar, G. Raju, Dr. Ch. Srinivasa Rao, Fabrication and Thermal Analysis of Composite Pin-Fin, International Journal of Core Engineering & Management. 77-89.

[27] W. Kowbel, C. A. Bruce, K.L. Tsou, K. Patel, and J.C. Withers and G.E. Youngblood, High Thermal Conductivity SiC/SiC Composites for Fusion Applications.